(1973); E. Valeo, C. Oberman, and F. W. Perkins, Phys. Rev. Lett. 28, 340 (1972); D. F. Dubois and M. V. Goldman, Phys. Rev. Lett. 28, 218 (1972).
[9]W. L. Kruer and J. M. Dawson, Phys. Fluids 15, 446 (1972); J. S. DeGroot and J. I. Katz, Phys. Fluids 16, 401 (1973).
[10]J. J. Thomson, R. J. Faehl, W. L. Kruer, and S. Bodner, Phys. Fluids 17, 973 (1974).
[11]J. S. DeGroot and J. E. Tull, University of California at Davis Report No. R-5, 1975 (unpublished).

Creation and Annihilation of Positive and Negative Pulses in an Unstable Macroplasma

Tetsuya Sato
Geophysics Research Laboratory, University of Tokyo, Tokyo 113, Japan
(Received 24 March 1975)

Repeated creation and annihilation of positive and negative pulses of spatially trapped particles are numerically observed as a result of nonlinear interactions in an extremely unstable macroplasma. Positive and negative pulses are successively created at opposite trapping boundaries and propagate toward each other with nearly constant speeds. Each pair of pulses collides and disappears at the center. New pulses are generated at shorter spacing, but propagate faster so that the time interval is nearly conserved.

In this Letter I wish to report a new phenomenon found through a two-dimensional numerical analysis of an unstable, magnetized macroplasma, namely, that positive and negative pulses of spatially trapped particles approach each other from opposite directions and collide to annihilate.

It is well known that trapped particles in a microplasma play an important role in the nonlinear evolution of an externally applied wave and of spontaneously excited unstable waves. Similarly it has recently been pointed out that the Hall motion induced by wave electric fields in a magnetized macroplasma (spatially trapped motion) also plays the leading role in the evolution of the waves.[1] Figure 1 illustrates electron trajectories in the phase space of a microplasma (top) and the Hall trajectories in the coordinate space perpendicular to the magnetic field (bottom) which are bounded in the direction perpendicular to the wave propagation direction. From this figure one may find points of similarity between the trapping motions in a microplasma and macroplasma, although the macroplasma has one isolated trapping region (vortex) for one wavelength but the macroplasma has two vortices.

I use a right-handed coordinate system in which a dc magnetic field B and a dc electric field E are applied along the positive x axis and the positive z axis, respectively. I treat a case in which electrons are almost collision free but ions are heavily dragged by neutrals. Consequently, only electrons drift toward the positive y axis. If the electron drift velocity exceeds the ion thermal speed, a two-stream instability results.[2] It is also known that a lower-frequency instability (cross-field instability) occurs for a condition in which the electron drift velocity is below the threshold of the two-stream instability, if the plasma density has a gradient in the direction parallel to the applied electric field.[3]

It has been shown[1] that these and other electrostatic macroinstabilities (e.g., the drift dissipative instability) are akin to one another and that their nonlinear development may generally be controlled by the spatially trapped particles. In this Letter I take up the cross-field instability, but the essential result may hold for other macroinstabilities.

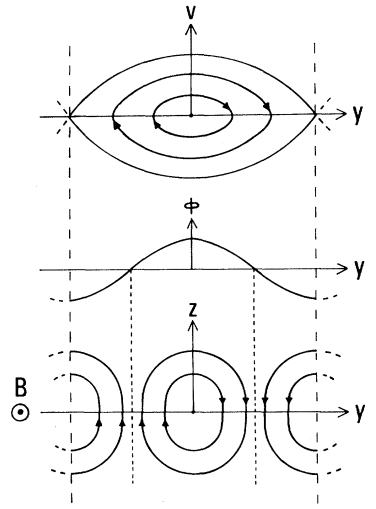

FIG. 1. Trapped particle trajectories in a potential wave (middle) for a microplasma (top) and for a magnetized macroplasma (bottom).

The governing equations to be solved are

$$\partial n/\partial t + \nabla_\perp \cdot n\vec{v}_{e\perp} = 0, \quad (1)$$

$$\nabla_\perp \cdot n(\vec{v}_{i\perp} - \vec{v}_{e\perp}) = 0, \quad (2)$$

where $n\vec{v}_{\alpha\perp} = \pm \mu_{P\alpha}\nabla_\perp\varphi = \mu_{H\alpha}\hat{z}\times\nabla_\perp\varphi - D_{\perp\alpha}\nabla_\perp n$ ($\alpha = e, i$), $\nabla_\perp$ is a gradient operator in the y-z plane, and $\hat{z}$ is the unit vector of the magnetic field; n is the electron density which is equal to the ion density because of charge neutrality, and φ is the electric potential; $\mu_{P\alpha}$, $\mu_{H\alpha}$, and $D_{\perp\alpha}$ are respectively the transverse (Pedersen) mobility, the Hall mobility, and the diffusion coefficient perpendicular to the magnetic field. I have assumed that the variables do not change in the direction of the magnetic field.

The geometry is such that the plasma is nonuniform along the z axis and bounded by two infinite planes put at $z = 0$ and $z = l$ which are kept at constant potentials, i.e., $\varphi = 0$ at $z = 0$ and $\varphi = -\varphi_0$ at $z = l$, but that the plasma is uniform and unbounded in the x and y directions.

I Fourier transform (1) and (2) with respect to y in the form

$$f(y,z,t) = \sum_{n=0}^{15} f_n(z,t)\exp(ink_m y),$$

where f stands for either n or φ and k_m corresponds to the wave number of the linearly most unstable mode. The Fourier-transformed equations are then transformed with respect to z to difference equations with equal intervals (31 meshes). The set of the Fourier-difference equations is then integrated with respect to time t by simply multiplying ΔT.[4]

The initial density distribution N^* was chosen to be in the form

$$N_* \equiv n_0(z, t=0) = \tfrac{1}{2}N_0[2.25 + 0.25\tanh 9\kappa l(z/l - 0.5)].$$

The initial perturbation was such that $n_n(z, t=0) = \epsilon N_* \sin(\pi z/l)$ for $n = 1$ and 0 otherwise.

Figure 2 is one numerical example that shows how the electron density distribution along the z axis, and hence the behavior of trapped particles, is modified by growing wave fields. R denotes the ratio of the applied electric field E ($=\varphi_0/l$) to the instability threshold, namely, a measure of the instability strength, and $\kappa l = 0.24$; $\epsilon = 0.01$ and $R = 10^4$. The time T is normalized by lB/E. Note that $R = 10^4$ implies an extremely unstable case.

As can be seen from Fig. 2, positive bumps (pulses) of trapped particles are successively born at the foot of the density hill and grow as they climb up the hill, while negative pulses are generated at the top of the hill (topside trapping boundary) and come down the hill. It should be stressed here that positive and negative pulses meet at about the trapping center ($z \simeq l/2$) and then disappear. It should also be noted that younger generations (newly born pulses) are sharper than older ones.

Trajectories of the peaks of positive and negative pulses are drawn in Fig. 3. The broken lines imply that the peaks are not clearly identifiable because of either small amplitudes or contamination of two pulses, so that it is not certain whether the trajectories are always straight or not. From this figure it is seen that the speed of a well-developed pulse, whether positive or negative, is constant and that spacing between two

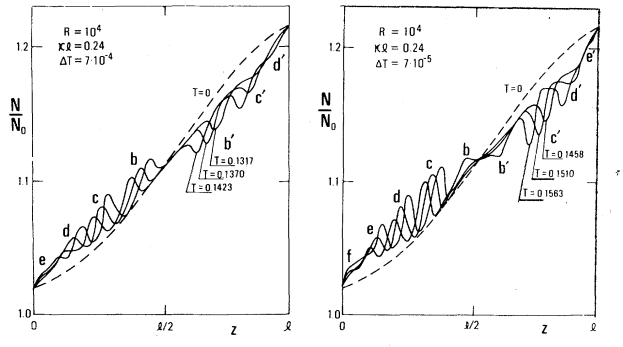

FIG. 2. Creation and annihilation of positive and negative pulse trains of trapped particles. Positive pulses (b, c, and d) run from left to right, while negative ones (b' and c') take the reverse way.

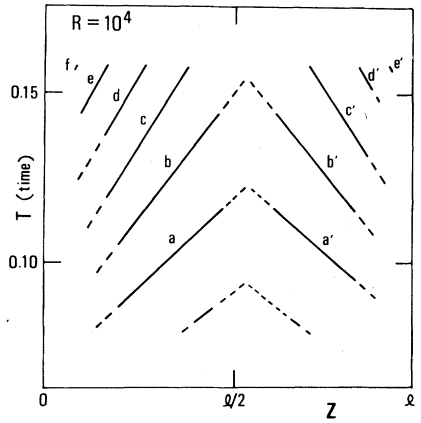

FIG. 3. Trajectories of positive ($a, \ldots, f$) and negative ($a', \ldots, e'$) pulses.

successive pulses becomes shorter and shorter; however, the time interval is nearly conserved. Accordingly, the collision time for a positive pulse and a negative pulse to meet and annihilate is also nearly constant. In other words, the speeds of newly born pulse pairs seem to be controlled so that the collision interval is rather conserved. Calculation has been made for $R = 200$, 50, 10, and 5. The above conclusion has been supported for $R = 200$ and 50. For $R = 10$ and 5, however, no conspicuous pulses are identified, but shocklike structures are formed near the trapping boundaries as shown in Fig. 4.

In Fig. 5 are shown the time evolutions of the amplitudes of the most unstable modes at $z = 10l/31$, $12l/31$, and $16l/31$ ($m = 10$, 12, and 16 in the figure). From this figure we may roughly say that the instability is saturated at about $T = 0.15$. It may be of value to note that many higher harmonic waves are excited and the turbulent energy spectrum reaches approximately $k^{-3.5}$. Similar calculations were performed by McDonald *et al.*[6] who obtained $k^{-3.5}$. Details of the turbulent structure and the results for other parameters ($R = 5$, 10, 50, and 200) will be published elsewhere.

Let us now derive a model equation which may represent the essential part of the observed result. The quasilinear equation governing the perturbed density distribution $n_0(z,t)$ can be given by[7]

$$\frac{\partial n_0(z)}{\partial t} \simeq A \frac{\partial n_k^2(z)}{\partial z} + D_{\perp a} \frac{\partial^2 n_0(z)}{\partial z^2}, \tag{3}$$

where $A = 2(\mu_{He}/\mu_{\perp i})(E/B)N_0^{-1} \approx 2\gamma/\kappa N_0$ and $D_{\perp a}$ is the ambipolar diffusion coefficient across the magnetic field, with μ_{He} and $\mu_{\perp i}$ the electron Hall mobility and the ion transverse mobility, respectively. Diffusion along the z axis is included because we are concerned with the variation along the z axis.

The equation of the wave energy can be expressed as[8]

$$\partial n_k^2(z)/\partial t = 2\gamma n_k^2(z) + D_{\perp a} \partial^2 n_k^2(z)/\partial z^2, \tag{4}$$

where γ is the quasilinear growth rate in which diffusion along the z axis is excluded, so that the diffusion term along z is separately added on the right-hand side. Although the diffusion is in general negligible, it must be taken into account when the fine structure along z is considered.

In addition, it is shown that when the wave amplitude grows sufficiently, the following relation roughly holds[9]:

$$\partial n_0^2(z)/\partial z \approx -\partial n_k^2(z)/\partial z. \tag{5}$$

Differentiating (3) once with respect to t, substituting (3) and (4), and making use of (5), I obtain

$$\frac{\partial^2 n_0}{\partial t^2} = -2\gamma A \frac{\partial n_0^2}{\partial z} - 2AD_{\perp\alpha} \frac{\partial^3 n_0^2}{\partial z^3} + D_{\perp\alpha} \frac{\partial^4 n_0}{\partial z^4}. \tag{6}$$

Introducing new dimensionless variables $\tilde{n}_0 = n_0(z)/N_0$, $\tau = t/t_0$, and $\xi = z/l$, with $t_0 = l/2AN_0 \simeq \kappa l/4\gamma$, (6) can be reduced to

$$\frac{\partial \tilde{n}_0}{\partial \tau} + \tilde{n}_0 \frac{\partial \tilde{n}_0}{\partial \xi} + \beta \frac{\partial^3 \tilde{n}_0^2}{\partial \xi^3} - \nu \frac{\partial^4 \tilde{n}_0}{\partial \xi^4} \simeq 0, \tag{7}$$

where $\beta = D_{\perp\alpha}/2\gamma l^2$ and $\nu = D_{\perp a}^2 t_0/2\gamma l^4$. In deriving (7) I have used the approximation that $\partial^2 n_0/\partial t^2 \approx 2\gamma \partial n_0/\partial t$ which can be obtained from (3) and (4) by neglecting the diffusion terms.

In the present numerical case $R = 10^4$, $\kappa l = 0.24$, $\beta \simeq 10^{-5}$, and therefore $\nu\beta^2\kappa l/2$ is approximately 10^{-11}. Since $|\tilde{n}_0| \approx 0.1$, we may omit the last term

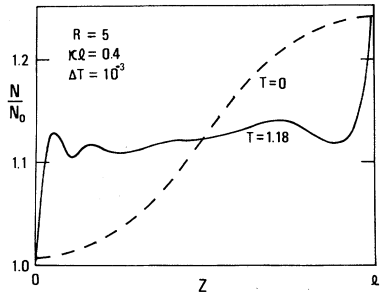

FIG. 4. Shocklike density profile deformed by trapped particles for a moderately unstable case (i.e., $R = 5$).

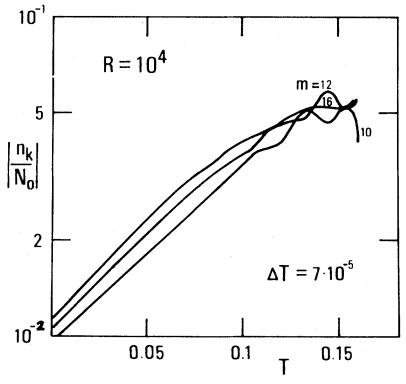

FIG. 5. Time evolution of the most unstable mode (k_m) at $z = 10l/31$ ($m = 10$), $12l/31$ ($m = 12$), and $16l/31$ ($m = 16$) for $R = 10^4$.

in (7). Thus, we obtain

$$\frac{\partial \tilde{n}_0}{\partial \tau}+\tilde{n}_0\frac{\partial \tilde{n}_0}{\partial \xi}+\beta\frac{\partial^3 \tilde{n}_0{}^2}{\partial \xi^3}=0. \quad (8)$$

From (8) we immediately notice that this equation is similar to the Korteweg–de Vries (kdV) equation[10] in a sense but differs in that the dispersion term is *nonlinear*. This difference is essential and significant.

In the KdV equation, positive and negative solitons cannot coexist. However, (8) is conserved for the replacement of $\tilde{n}_0$ with $-\tilde{n}_0$ and τ (or ξ) with $-\tau$ (or $-\xi$). Therefore, (8) allows negative pulses which propagate in the opposite direction. Another important difference is that invariants are present with respect to *odd* powers of $\tilde{n}_0$ but *not* with respect to even powers of $\tilde{n}_0$. This character may be understabdable because $\tilde{n}_0$ is the density. The total density is conserved but the square of the total density should not be conserved in general. From this fact it is possible that a positive pulse of $\tilde{n}_0$ and a negative pulse with the same shape may annihilate when they encounter.

Now we seek a steady solution of (8) in the form $\tilde{n}_0(\xi,\tau)=\tilde{n}_0(\xi-c\tau)$, where c is a constant. Integrating twice with respect to $\eta\equiv\xi-c\tau$ yields

$$(\partial\tilde{n}_0/\partial\eta)^2=(8\beta)^{-1}\tilde{n}_0(\tfrac{1}{3}8c-\tilde{n}_0). \quad (9)$$

Equation (9) is solved to give

$$n_0=\tfrac{8}{3}c\cos^2[\xi-2(\mu_{He}/\mu_{\perp i})cT]/4(2\beta)^{1/2}, \quad (10)$$

where another normalized time T $(=tE/Bl)$ is used to make it possible to compare with numerical results in which this normalized time is used (see for example Fig. 3). From (10) it can be seen that the pulse speed is proportional to its amplitude and given by $2(\mu_{He}/\mu_{\perp i})c$ and that the pulse interval is about $4\pi(2\beta)^{1/2}l$. Since $(\mu_{He}/\mu_{\perp i})$ was chosen to be 25 in the numerical case and c (relative density wave amplitude) is about 0.1, the pulse speed is expected to be $5l$ which is in good agreement with the observed pulse speeds (Fig. 3). The pulse distance becomes about $0.06l$ which is also in agreement with numerical results (see Fig. 2).

It may be of value to note that physically the pulse speed is the electron Hall speed driven by the wave electric field.

I wish to thank Dr. T. Ogawa for his help in computation. Part of this work was conduced while I belonged to the Department of Physics, Kyoto University. The Institute of Plasma Physics, Nagoya University, is acknowledged for partial financial support for the computation.

[1]T. Sato, Phys. Fluids 17, 621 (1974).
[2]D. T. Farley, Phys. Rev. Lett. 10, 279 (1963).
[3]A. Simon, Phys. Fluids 6, 382 (1963).
[4]T. Sato and T. Ogawa, Phys. Fluids 17, 628 (1974).
[5]T. Sato, Phys. Fluids 14, 2426 (1971); T. Sato, T. Ogawa, and Y. Matsuda, Phys. Fluids 15, 1926 (1972).
[6]B. E. McDonald, T. P. Coffey, S. Ossakow, and R. N. Sudan, J. Geophys. Res. 79, 2551 (1974).

[7]Equation (14) in Ref. 1 is rewritten, with the use of Eq. (13), as

$$\frac{\partial n_0}{\partial t}=2k_y\frac{M}{M_\perp}\frac{\partial}{\partial z}\frac{\sin\psi}{a}n_k{}^2.$$

By using Eq. (50) in Ref. 1 and the approximation $M/M_\perp\simeq\mu_{He}$, this can be reduced to $\partial n_0/\partial t\simeq A\partial n_k{}^2/\partial z$. Since the ambipolar diffusion along z was neglected in Ref. 1, we must add this diffusion to the right-hand side. Thus Eq. (3) of this work is obtained.

[8]The density fluctuation n_k is generally expressed as $n_k=\bar{n}_k\exp(-i\omega_r t+i\vec{k}\cdot\vec{x}+\gamma t)$. Thus $n_k{}^2=\bar{n}_k{}^2\exp(2\gamma t)$, namely, $\partial n_k{}^2/\partial t=2\gamma n_k{}^2$. Since in general diffusion along z is included in γ, this term can be separated out. Then (4) is derived.

[9]See Eqs. (57) and (58) in Ref. 1.

[10]N. J. Zabusky and M. D. Kruskal, Phys. Rev. Lett. 15, 240 (1965); R. M. Miura, C. S. Gardner, and M. D. Kruskal, J. Math. Phys. (N. Y.) 9, 1204 (1968).